

## The Effect of Pregnenolone 16 $\alpha$ -Carbonitrile on the Pharmacokinetics and Metabolism of Dapsone in Rats

MING LU, SAMUEL M. POLOYAC, PATRICK J. MCNAMARA AND ROBERT A. BLOUIN

*University of Kentucky, College of Pharmacy, Rose St., Lexington, KY 40536-0082, USA*

### Abstract

The purpose of this study was to evaluate the effect of pregnenolone 16 $\alpha$ -carbonitrile (PCN) on the interconversion pharmacokinetics and metabolism of dapsone. To determine microsomal CYP3A activity and protein, eight rats (4 PCN, 4 corn oil) received a 1 mg kg<sup>-1</sup> intravenous bolus dose of dapsone, followed by blood and urine sampling. The formation clearance of dapsone hydroxylamine (CL<sub>f</sub> DDS-NOH) was calculated from the obtained samples. Interconversion pharmacokinetics estimates were obtained after 10 rats (5 PCN, 5 control) received 1 mg kg<sup>-1</sup> dapsone or 1.17 mg kg<sup>-1</sup> monoacetyldapsone, with a 24-h wash-out.

Results from the interconversion analysis demonstrated that PCN significantly increased systemic clearance (CL<sub>s</sub>) of dapsone, but not its interconversion. The in-vivo/in-vitro correlation study demonstrated that PCN significantly increased CL<sub>s</sub> of dapsone (8.55 to 16.39 mL min<sup>-1</sup>;  $P < 0.01$ ) and CL<sub>f</sub> DDS-NOH (0.13 to 0.18 mL min<sup>-1</sup>;  $P < 0.01$ ). PCN treatment produced a 69% increase in CYP3A protein, and increased 6 $\beta$ - and 2 $\beta$ -hydroxytestosterone formation rates. Significant correlations were found between CL<sub>f</sub> DDS-NOH and either 6 $\beta$ - ( $r^2 = 0.925$ ), 2 $\beta$ -hydroxytestosterone ( $r^2 = 0.92$ ), or CYP3A1/2 protein ( $r^2 = 0.60$ ).

We conclude that PCN treatment produces significant increases in CL<sub>s</sub> (dapsone) and CL<sub>f</sub> (DDS-NOH) in rats. These changes were not due to changes in the reversible metabolism of dapsone. These results suggest that the formation clearance of dapsone hydroxylamine reflects alterations in CYP3A activity, despite the fact that it accounted for a small part of the systemic clearance of dapsone.

Therapeutic applications of dapsone have expanded since it was first discovered for the treatment of leprosy 40 years ago (Zuidema et al 1986). These include the treatments for malarial prophylaxis (Powell et al 1967), autoimmune diseases (Grindulis & McConkey 1984), and more recently for Kaposi's sarcoma (Poulsen et al 1984) and *Pneumocystis carinii* (Lee et al 1993) in AIDS patients. However, there is still limited knowledge of the pharmacokinetic characteristics of dapsone despite its long history. In man, dapsone exhibits a long half-life, multiple metabolic pathways, and metabolite-related haematological toxicity. Although the metabolic profile of dapsone (Orzech et al 1976) is rather complicated in man, its major hepatic metabolic pathways are N-oxidation and N-

acetylation (Figure 1). Once absorbed, dapsone is either N-hydroxylated to form dapsone hydroxylamine (DDS-NOH) or N-acetylated to form monoacetyldapsone (MADDS), followed by Phase II conjugation reactions. Dapsone shows a moderate 70% of protein binding in man. The large volume of distribution and similar dapsone concentration between plasma and tissue indicates the extensive distribution of dapsone.

The hydroxylation pathway is believed to be responsible for the adverse reactions of dapsone, such as methaemoglobinaemia and haemolysis. Both DDS-NOH and monoacetyldapsone hydroxylamine are capable of inducing methaemoglobin formation (Cucinell et al 1972; Vage et al 1994). The N-hydroxylation of dapsone is mediated by cytochrome P450. Cimetidine, a cytochrome P450 inhibitor, has been shown in man and rats to inhibit the formation of hydroxylamines and as a result, prevents the formation of methaemoglobin

Correspondence: R. A. Blouin, Division of Pharmaceutical Sciences, College of Pharmacy, University of Kentucky, Rose St, Lexington, KY 40536-0082, USA.  
E-Mail: rblou1@pop.uky.edu

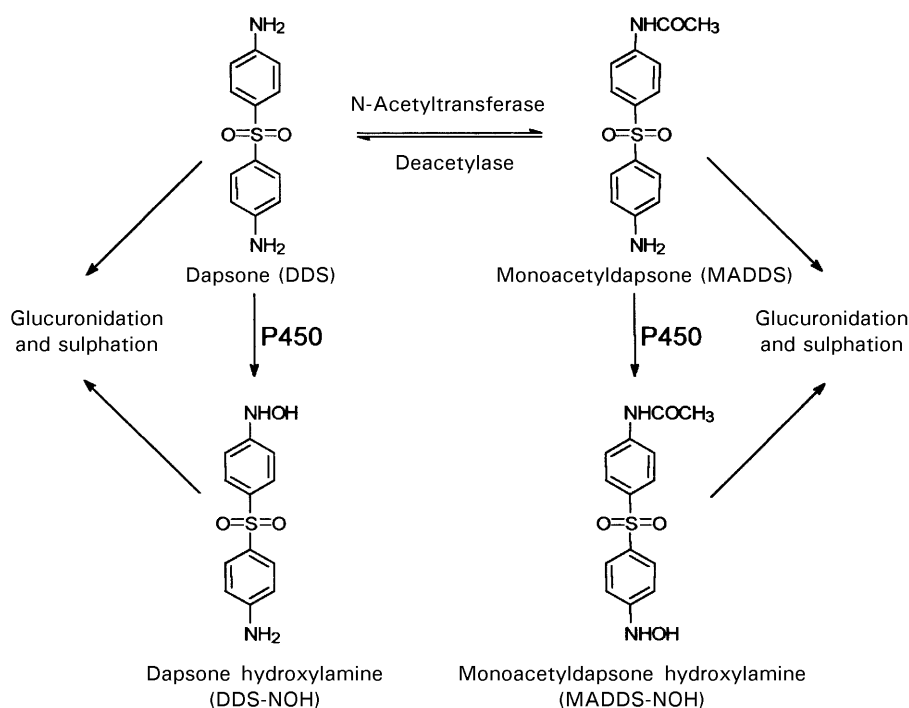


Figure 1. The N-oxidation and N-acetylation of dapsone. All of these four compounds can be conjugated to glucuronides and sulphates.

(Coleman et al 1990a, b, 1991). However, studies evaluating the specific P450s involved in this reaction have produced conflicting results. Fleming et al (1992) suggested that dapsone was predominantly metabolized by human hepatic CYP3A4, and proposed dapsone as a non-invasive in-vivo probe of CYP3A4. Kinirons et al (1993) found no correlation between dapsone recovery ratio with two other CYP3A probes, erythromycin breath test, and cortisol recovery ratio. Furthermore, other cytochrome P450s appeared to be involved, CYP2C6/2C11 in rats (Vage & Svensson 1994), and CYP2E1 (Mitra et al 1995) and CYP2C9 in man (Gill et al 1995). Most recently, a new unidentified metabolite was found and it was possibly formed by CYP3A (Irshaid et al 1996).

The pharmacokinetics of dapsone is further complicated by the reversible nature of the N-acetylation pathway. Dapsone is biotransformed to MADDS by arylamine N-acetyltransferase (Hein 1988). The formed MADDS can then be converted back to dapsone by the deacetylase simultaneously. This interconversion has been found in rats (Gordon et al 1975), rabbits (Pochopin et al 1994) and man (Gelber et al 1971). Classical pharmacokinetic analysis provides limited insight into the individual metabolic pathways involved, because the interconversion process and elimination of metabolite also affect the apparent

pharmacokinetic parameters calculated by the traditional methods.

Moreover, hydroxylation and acetylation are apparently interrelated. Glucocorticoids (Zaher & Svensson 1994), pyrimethamine (Palamanda et al 1995), folate (Coleman et al 1996), isoniazid and sulphamethazine (Ahmad et al 1981) reportedly affected the interconversion between dapsone and MADDS via regulation of the activities of N-acetyltransferase, thereby producing a shift in the P450-mediated formation of toxic hydroxylamines. However, the effects of drug interactions or disease states on the reversible metabolism of dapsone have not been studied thoroughly. These evaluations are hampered by the complexity of reversible metabolism analysis (Ebling & Jusko 1986).

As the most abundant cytochrome P450 isoform and the major drug-metabolizing enzyme in human liver and intestine, CYP3A may explain many cytochrome P450-mediated toxic reactions and drug interactions of dapsone. Therefore, the purpose of this study was to investigate the pharmacokinetics and drug metabolism of dapsone following CYP3A induction by PCN. The interrelationship between N-hydroxylation and N-acetylation was then interpreted by reversible metabolism analysis. In addition, the effect of PCN on elimination of dapsone in rats was examined by use of an in-vivo/in-vitro study.

## Materials and Methods

### Chemicals

Dapsone, NADP, glucose 6-phosphate, glucose 6-phosphate dehydrogenase, 50% Tris-buffered saline with 0.1% Tween 20, and phosphate carbonate/bicarbonate buffered saline (pH 9.6) were purchased from Sigma (St Louis, MO). 3-Aminophenyl sulphone was obtained from Aldrich (Milwaukee, WI). Testosterone and its hydroxyl metabolites were purchased from Steraloid Inc. (Wilton, NH). Monoacetyldapsone was a gift from Parke-Davis (Ann Arbor, MI). Microsomal standard and polyclonal goat anti-rat antibody for CYP3A1/2 were obtained from Gentest (Woburn, MA). *p*-Nitrophenol phosphate substrate was supplied by ELISA Technologies (Lexington, KY). Dapsone hydroxylamine was synthesized in our laboratory with no significant impurities observed according to HPLC or NMR evaluation.

### Animals

Male Sprague-Dawley rats (200–300 g) were purchased from Harlan Industries (Indianapolis, IN). The rats were randomly assigned to PCN treatment (i.p. 50 mg/day for 3 days) or control (corn oil, i.p. 3.3 mL kg<sup>-1</sup>/day for 3 days) groups. On day 3, the rats were implanted with a jugular vein catheter and allowed 24 h to recover.

### The in-vivo/in-vitro correlation study

Eight rats (4 PCN and 4 control) received an intravenous bolus dose of dapsone (1 mg kg<sup>-1</sup>) followed by serial blood samples at 20 min, 40 min, 1, 2, 4, 6, 9, 12 and 24 h. Throughout the entire sample period, the rats were housed in Nalgene metabolism cages and 24-h urine samples were collected in a container with 1 g ascorbic acid. The urine samples were then stored at -80°C. The analysis of plasma dapsone concentration was adopted from Irshaid et al (1994) with a detection limit of 5 ng mL<sup>-1</sup>. The urine samples were hydrolysed in the presence of hydrochloric acid, and dapsone hydroxylamine was then quantified by the method of May et al (1990) with a detection limit of 25 ng mL<sup>-1</sup>. Both assays used 3-aminophenyl sulphone as the internal standard.

Following the 24-h blood samples, the rats were killed and liver microsomes prepared by a differential centrifugation method (Lu & Levin 1972). The pellets were resuspended in 0.25 M sucrose and stored at -80°C. The protein concentrations of microsomal preparations were then determined by the method of Lowry et al (1951). The in-vitro

cytochrome P450 activities were evaluated by the testosterone substrate assay (Sonderfan et al 1987).

CYP3A1/2 protein concentrations were determined by non-competitive enzyme-linked immunosorbant assay (ELISA). Liver microsomes were diluted in phosphate carbonate/bicarbonate buffered saline (pH 9.6) (Sigma; St Louis, MO). Subsequently, 0.25 µg of total microsomal sample protein and known concentration of microsomal standard were plated onto 96-well flat-bottom plates (Corning, NY). Proteins were blocked and incubated with 50% horse serum and 50% Tris buffered saline with 0.1% Tween 20. The plates were then washed and incubated with polyclonal goat anti-rat antibody for CYP3A1/2. The plates were washed and incubated with alkaline phosphatase conjugated monoclonal rabbit anti-goat IgG antibody. After this incubation, the plates were washed and *p*-nitrophenol phosphate substrate was added. The plates were analysed at 405 nm over 30 min at 37°C with a Biotek EL340 microplate reader for colour formation. The CYP3A1/2 concentrations of liver microsomal samples were determined from the fitted standard curve.

### The reversible metabolism study

Ten rats were randomly assigned to receive either PCN or corn oil treatment (5 PCN, 5 control) for three days. Utilizing a balanced crossover design,

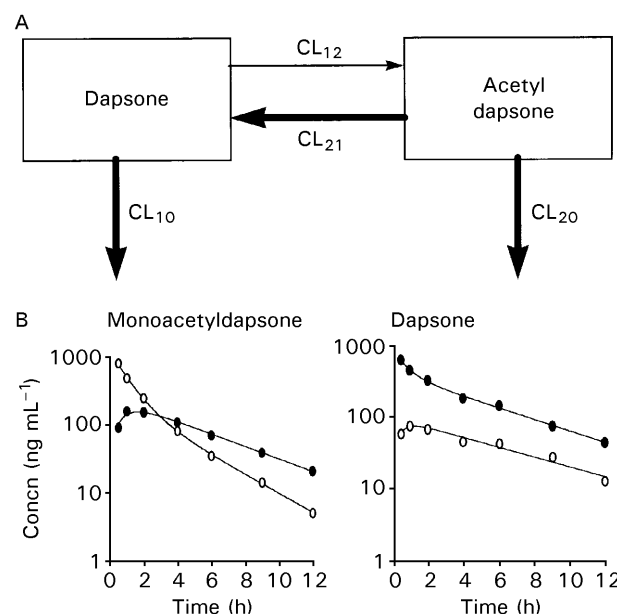


Figure 2. A. The interconversion model for dapsone. CL<sub>12</sub> and CL<sub>21</sub> are the acetylation and deacetylation clearances, respectively. CL<sub>10</sub> and CL<sub>20</sub> are the clearances of dapsone and MADDs, respectively. B. Representative plasma concentration-time profiles for dapsone (●) and monoacetyldapsone (○) after intravenous administration of 1.17 mg kg<sup>-1</sup> monoacetyldapsone or 1 mg kg<sup>-1</sup> dapsone.

each rat was given intravenous dapsone ( $1 \text{ mg kg}^{-1}$ ) and an equal molar dose of monoacetyldapsone ( $1.17 \text{ mg kg}^{-1}$ ), separated by a 24-h wash-out. Following each dose, 0.3 mL blood was removed at 0.5, 1, 2, 4, 6, 9 and 12 h, with an equal volume of physiological saline injected to replace blood volume loss. Plasma samples were then stored at  $-20^\circ\text{C}$  until analysis for dapsone and MADDs.

Reversible metabolism analysis was calculated by the simple interconversion model (Figure 2A) proposed by Ebling & Jusko (1986). The following equations were used to calculate the individual interconversion clearance values for dapsone.

$$CL_{10} = \frac{D^p \bullet AUC_m^m - D^m \bullet AUC_m^p}{AUC_p^p \bullet AUC_m^m - AUC_m^p \bullet AUC_p^m} \quad (1)$$

$$CL_{12} = \frac{D^m \bullet AUC_p^p}{AUC_p^p \bullet AUC_m^m - AUC_m^p \bullet AUC_p^m} \quad (2)$$

$$CL_{20} = \frac{D^m \bullet AUC_p^p - D^p \bullet AUC_p^m}{AUC_p^p \bullet AUC_m^m - AUC_m^p \bullet AUC_p^m} \quad (3)$$

$$CL_{12} = \frac{D^p \bullet AUC_p^m}{AUC_p^p \bullet AUC_m^m - AUC_m^p \bullet AUC_p^m} \quad (4)$$

$$CL_{\text{real}}^p = CL_{10} + CL_{12} \quad (5)$$

$$CL_{\text{real}}^m = CL_{20} + CL_{21} \quad (6)$$

$$CL_S^p = \frac{D^p}{AUC_p^p} = CL_{10} + \frac{CL_{12} \bullet CL_{20}}{CL_{21} + CL_{20}} \quad (7)$$

$$CL_S^m = \frac{D^m}{AUC_m^m} = CL_{20} + \frac{CL_{21} \bullet CL_{10}}{CL_{12} + CL_{10}} \quad (8)$$

$$EE = \frac{CL_{\text{real}}^p}{CL_{\text{app}}^m} \quad (9)$$

Where  $CL_{12}$  is the acetylation clearance,  $CL_{21}$  the deacetylation clearance,  $CL_{10}$  and  $CL_{20}$  are total clearance of drug and MADDs excluding interconversion.  $D^p$  is the dose of the parent drug administrated to rats and  $D^m$  is the dose of metabolite. For AUC, superscript refers to the substance being administered and subscript refers to the concentration of substance being measured. For example,  $AUC_m^p$  is the area under the curve of metabolite following administration of the parent drug.  $CL_S$  is the apparent clearance without considering interconversion, while  $CL_{\text{real}}$  is the real clearance calculated by interconversion analysis. EE, the exposure enhancement, measures the ratio

of AUC with interconversion over AUC without interconversion.

#### Pharmacokinetic and statistical analysis

Pharmacokinetic analysis of dapsone and MADDs was performed by PKAnalyst (version 1.1, Micro-Math Inc.). The concentration–time data of the parent compounds and the formed metabolites were best fitted to a biexponential function. The values of area under curve ( $AUC_{0-\infty}$ ) and area under moment curve ( $AUMC_{0-\infty}$ ) were then obtained from the slope–intercept method. The following pharmacokinetic parameters were then calculated: clearance ( $CL_s = \text{DOSE}_{i.v.}/AUC$ ), formation clearance of dapsone hydroxylamine ( $CL_f = f_{m,u}CL_s$ ), and volume of distribution ( $Vd_{ss} = \text{DOSE}_{i.v.} \bullet AUMC/AUC^2$ ).

Unpaired Student's *t*-test was used to compare PCN treatment and control groups. Statistical significance was declared if  $P < 0.05$ . Least-square regression was used to analyse the possible relationship between in-vivo formation clearance of dapsone hydroxylamine and in-vitro hepatic CYP3A protein content and activity.

## Results

#### Reversible metabolism

Typical plasma concentration–time profiles for dapsone and MADDs in the same rats are presented in Figure 2B. Pharmacokinetic parameters generated using the interconversion model are listed in Table 1. PCN treatment produced a statistically significant 29% increase in  $CL_{10}$  ( $P < 0.05$ ). Although a 33% increase in  $CL_{20}$  was observed, this trend did not reach statistical significance. Neither interconversion clearances,  $CL_{12}$  nor  $CL_{21}$ , were significantly altered as a consequence of PCN treatment. No change was seen in exposure

Table 1. Pharmacokinetic and interconversion parameters of dapsone and monoacetyldapsone following intravenous injection of dapsone ( $1 \text{ mg kg}^{-1}$ ) and monoacetyldapsone ( $1.17 \text{ mg kg}^{-1}$ ) in PCN-induced and control rats.

Kinetic parameters	Control	PCN treatment
$CL_{10}$ ( $\text{mL min}^{-1} \text{ kg}^{-1}$ )	$5.65 \pm 0.54$	$7.29 \pm 1.18^*$
$CL_{12}$ ( $\text{mL min}^{-1} \text{ kg}^{-1}$ )	$3.13 \pm 0.54$	$3.27 \pm 0.84$
$CL_{20}$ ( $\text{mL min}^{-1} \text{ kg}^{-1}$ )	$10.31 \pm 2.36$	$13.74 \pm 5.54$
$CL_{21}$ ( $\text{mL min}^{-1} \text{ kg}^{-1}$ )	$6.54 \pm 1.01$	$8.51 \pm 4.06$
$CL_{\text{real}}^p$ ( $\text{mL min}^{-1} \text{ kg}^{-1}$ )	$8.77 \pm 0.93$	$10.56 \pm 1.68^*$
$CL_{\text{app}}^p$ ( $\text{mL min}^{-1} \text{ kg}^{-1}$ )	$7.57 \pm 0.83$	$9.29 \pm 1.18$
EE	$1.16 \pm 0.02$	$1.13 \pm 0.05$

Values are the mean  $\pm$  s.d. of five rats.  $*P < 0.05$ , unpaired-*t*-test for comparison between control and PCN-induced groups.

enhancement (EE), which represents the degree of conservation due to metabolic recycling.

#### *In-vivo/in-vitro studies*

Figure 3 shows the typical concentration–time profiles of dapsone following intravenous administration of  $1 \text{ mg kg}^{-1}$  dapsone in the control and PCN-induced rats. Dapsone concentration–time profiles after the intravenous injection were best fitted to a biexponential function. PCN treatment significantly reduced the AUC of dapsone but did not alter the terminal half-life of dapsone. As shown in Table 2, PCN treatment significantly increased dapsone clearance ( $CL_s$ ;  $8.55$  to  $16.39 \text{ mL min}^{-1}$ ,  $P < 0.01$ ) and formation clearance of dapsone hydroxylamine ( $CL_f$ ;  $0.13$  to  $0.18 \text{ mL min}^{-1}$ ,  $P < 0.01$ ). The fraction of the dose excreted as the DDS-NOH was calculated as  $1.53 \pm 0.11\%$  in control and  $1.13 \pm 0.27\%$  in PCN-treated animals. The PCN group showed an unexpected 48% increase in the  $V_{d_{ss}}$  of dapsone ( $P < 0.01$ ).

The in-vitro studies were performed on microsomes from individual rats. Table 2 shows that PCN treatment resulted in a 69% increase in apparent liver CYP3A protein concentrations and

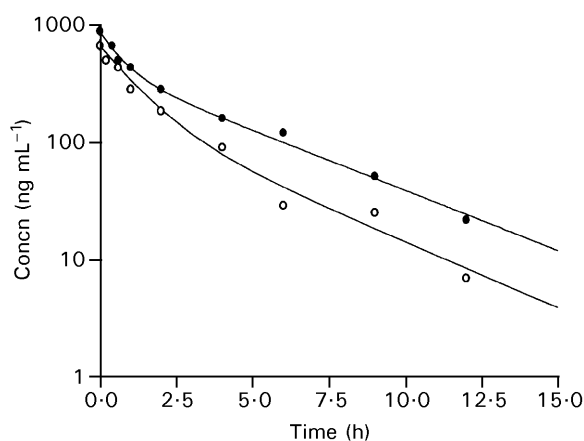


Figure 3. The plasma concentration–time profiles of dapsone following intravenous administration of  $1 \text{ mg kg}^{-1}$  dapsone in PCN-induced (○) and control (●) rats.

Table 2. The in-vivo pharmacokinetic parameters of dapsone following intravenous injection of dapsone and in-vitro CYP3A1/2 activity and protein content of hepatic microsomes in PCN-induced and control rats.

Treatment		Control	PCN induction
In-vivo study	$CL_s$ ( $\text{mL min}^{-1} \text{ kg}^{-1}$ )	$8.55 \pm 0.99$	$16.39 \pm 3.05^\dagger$
	$CL_f$ ( $\text{mL min}^{-1} \text{ kg}^{-1}$ )	$0.13 \pm 0.01$	$0.18 \pm 0.20^\dagger$
	$V_{d_{ss}}$ ( $\text{L kg}^{-1}$ )	$1.68 \pm 0.01$	$2.49 \pm 0.36^\dagger$
In-vitro study	$2\beta$ -Hydroxytestosterone ( $\text{pmol mg}^{-1} \text{ min}^{-1}$ )	$127 \pm 28$	$606 \pm 159^\dagger$
	$6\beta$ -Hydroxytestosterone ( $\text{pmol mg}^{-1} \text{ min}^{-1}$ )	$932 \pm 188$	$2719 \pm 595^\dagger$
	CYP3A1/2 protein ( $\text{pmol (mg protein)}^{-1}$ )	$146 \pm 5.8$	$246 \pm 44.8^\dagger$

Values are the mean  $\pm$  s.d. of four rats.  $^\dagger P < 0.01$  *t*-test for comparison between PCN induction and control groups.

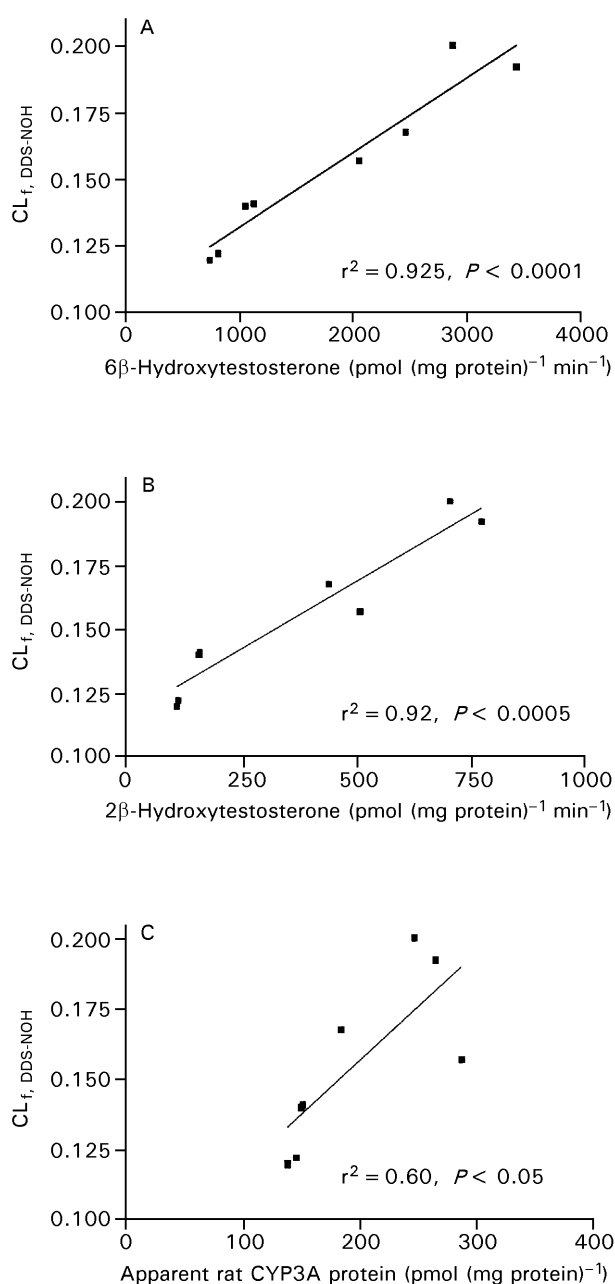


Figure 4. The correlation between the in-vivo formation clearance of dapsone hydroxylamine ( $CL_f$ ) and  $6\beta$ -hydroxytestosterone (A),  $2\beta$ -hydroxytestosterone (B), and apparent CYP3A protein level (C).

increases in the formation rate of  $6\beta$ -hydroxytestosterone and  $2\beta$ -hydroxytestosterone (three- and fivefold, respectively). The PCN-induction of CYP3A corresponded with the increase in formation clearance of dapson hydroxylamine. Figure 4 shows a significant correlation between formation clearance ( $CL_f$ ) and  $6\beta$ -hydroxytestosterone ( $r^2 = 0.925$ ),  $2\beta$ -hydroxytestosterone ( $r^2 = 0.92$ ) and CYP3A1/2 protein ( $r^2 = 0.60$ ).

### Discussion

PCN treatment significantly increased  $CL_s$  and  $CL_f$  (Table 2). The magnitude of the increase in  $CL_s$  cannot be solely accounted for by the N-hydroxylation pathway.  $CL_f$  constituted less than 2% of  $CL_s$ . The metabolic pathways of hepatic metabolism of dapson include hydroxylation, acetylation, sulphation and glucuronidation (Figure 1). The lipophilic character of the acetylated metabolite does not allow for the subsequent renal elimination of MADDs in the urine due to a large degree of renal tubular reabsorption in man (Israili et al 1973; Coleman et al 1990b). Therefore, MADDs itself is predominant in the plasma but is not appreciably excreted in the urine unless hydroxylation, glucuronidation or sulphation occur. Despite the requirement of additional metabolism in the excretion of acetylated dapson metabolites, this pathway contributed 21 to 34% of the apparent clearance of dapson in the rat.

The interconversion analysis (Table 1) indicated that PCN did not cause a significant change in the interconversion clearances or MADDs clearance. PCN has been reported to induce not only CYP3A1 (Williams et al 1994) but also uridine diphosphate-glucosyltransferase (Arlotto et al 1987). Although CYP3A activity increased several fold, N-hydroxylation made a very small contribution to the  $CL_s$ . Therefore, the unaccounted change of  $CL_s$  was probably the result of enhanced glucuronidation of dapson. In addition, the lack of alteration in MADDs clearance would suggest that N-hydroxylation of MADDs is unaffected by PCN. This data is in agreement with that of Coleman et al (1991) who demonstrated that MADDs N-hydroxylation was not blocked by cimetidine administration, thereby suggesting the involvement of other P450 isoforms in the hydroxylation of the monoacetylated metabolite.

The limitations of using dapson systemic clearance or urinary excretion as an in-vivo tool to assess functional clearance via a particular enzyme are the presence of multiple metabolic pathways and reversible metabolism of dapson. As discussed, the apparent clearance of dapson is due to

the combination of  $CL_{10}$ ,  $CL_{20}$ ,  $CL_{12}$  and  $CL_{21}$ . Perturbing either the N-hydroxylation or interconversion pathways may lead to a change in the apparent clearances of dapson and the fraction of the dose eliminated as dapson hydroxylamine; therefore, use of these terms to evaluate dapson hydroxylation can be misleading. However, this dilemma can be addressed by using the formation clearance of dapson hydroxylamine ( $CL_f$ ).

A distinct advantage in the use of  $CL_f$  to estimate the extent of elimination down a particular metabolic pathway is the independent nature of the parameter. Like renal clearance, formation clearance provides a functional estimate of a clearance mechanism that is not influenced by changes in competing pathways. Formation clearance is also valid for the situation involving metabolic interconversion, as is the case for dapson. On a theoretical basis, and as verified using computer simulations of the model depicted in Figure 5, formation clearance is not biased by changes in the interconversion pathways caused by PCN induction. Hence,  $CL_f$  is proportional to the capacity of the N-hydroxylation pathway, but independent of the interconversion or glucuronidation pathways. For drugs with a low extraction ratio such as dapson,  $CL_f$  reflects the intrinsic activity of hydroxylation enzymes. That was proven by the high in-vivo/in-vitro correlations between  $CL_f$  and CYP3A protein level and activity. Therefore, if accurately measured, the formation clearance of dapson hydroxylamine will be a useful tool for predicting hepatic CYP3A activity in rats despite being a minor pathway for dapson elimination.

The effect of PCN on dapson pharmacokinetics is more complex than initially expected. For drugs with reversible metabolism, their volume of distribution at steady state is dependent on plasma-protein

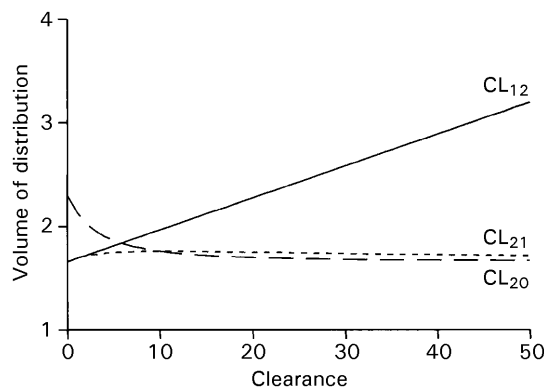


Figure 5. The effect of clearances of interconversion ( $CL_{12}$ ,  $CL_{21}$ ) and monoacetyldapson ( $CL_{20}$ ) on the apparent volume of distribution of dapson at steady state. The simulation is based on mean interconversion parameters of dapson from control rats.

binding, tissue binding, and interconversion clearances. In this study, PCN was found to increase the  $V_{d_{ss}}$  of dapsone. Coincidentally, troleandomycin, a CYP3A inhibitor, was found to decrease the  $V_{d_{ss}}$  of methylprednisolone in a study evaluating the reversible metabolism of methylprednisolone (Ebling et al 1987). The authors suggested that it might have been caused by the change in the interconversion of methylprednisolone (Cheng & Jusko 1993). Based on the report that N-acetyltransferase was induced in dexamethasone-treated rats (Zaher & Svensson 1994), we suggested that PCN might induce N-acetyltransferase activity and acetylation clearance of dapsone. The effect of  $CL_{12}$ ,  $CL_{21}$ , and  $CL_{20}$  on apparent  $V_{d_{ss}}$  of dapsone is illustrated in Figure 5, which shows that the acetylation clearance  $CL_{12}$  has the most influence on the value of apparent  $V_{d_{ss}}$ . However, our data did not support the interconversion theory. Reversible metabolism analysis in this study demonstrated that PCN treatment did not alter the interconversion clearances,  $CL_{12}$  and  $CL_{21}$ .

This study indicated that PCN treatment increased the systemic clearance of dapsone and the formation clearance to the hydroxylamine in the rat. In addition, the in-vivo formation clearance of dapsone hydroxylamine was highly correlated with in-vitro CYP3A activity and protein, despite the fact that it accounts for a very small portion of the total systemic clearance. The increase in systemic clearance of dapsone, which cannot be explained by CYP3A induction, might be caused by a PCN-induced glucuronidation pathway. The interconversion analysis showed that the acetylation pathway contributed a significant percentage of the total clearance of dapsone in rats. The data provided here may aid in the future characterization of drug interactions and disease states, which influence the disposition of dapsone.

## References

- Ahmad, R. A., Rogers, H. J., Vandenburg, M., Wright, P. (1981) Effects of concurrent administration of other substrates of N-acetyltransferase on dapsone acetylation. *Br. J. Clin. Pharmacol.* 12: 83–86
- Arlotto, M. P., Sonderfan, A. J., Klaassen, C. D., Parkinson, A. (1987) Studies on the pregnenolone-16 alpha-carbonitrile-inducible form of rat liver microsomal cytochrome P-450 and UDP-glucuronosyltransferase. *Biochem. Pharmacol.* 36: 3859–3866
- Cheng, H., Jusko, W. J. (1993) Pharmacokinetics of reversible metabolic systems. *Biopharm. Drug. Dispos.* 14: 721–766
- Coleman, M. D., Hoaksey, P. E., Breckenridge, A. M., Park, B. K. (1990a) Inhibition of dapsone-induced methaemoglobinaemia in the rat isolated perfused liver. *J. Pharm. Pharmacol.* 42: 302–307
- Coleman, M. D., Scott, A. K., Breckenridge, A. M., Park, B. K. (1990b) The use of cimetidine as a selective inhibitor of dapsone N-hydroxylation in man. *Br. J. Clin. Pharmacol.* 30: 761–767
- Coleman, M. D., Tingle, M. D., Park, B. K. (1991) Inhibition of dapsone induced methaemoglobinaemia by cimetidine in the rat during chronic dapsone administration. *J. Pharm. Pharmacol.* 43: 186–190
- Coleman, M. D., Pahal, K. K., Gardiner, J. M. (1996) The effect of acetylation and deacetylation on the disposition of dapsone and monoacetyl dapsone hydroxylamines in human erythrocytes in-vitro. *J. Pharm. Pharmacol.* 48: 401–406
- Cucinell, S. A., Israeli, Z. H., Dayton, P. G. (1972) Microsomal N-oxidation of dapsone as a cause of methemoglobin formation in human red cells. *Am. J. Trop. Med. Hyg.* 21: 322–333
- Ebling, W. F., Jusko, W. J. (1986) The determination of essential clearance, volume, and residence time parameter of recirculating metabolic systems: the reversible metabolism of methylprednisolone and methylprednisone in rabbits. *J. Pharmacokinet. Biopharm.* 14: 557–599
- Ebling, W. F., Rich, S. A., Szefer, S. J., Jusko, W. J. (1987) Troleandomycin effects on methylprednisolone and methylprednisone interconversion and disposition in the rabbit. *Eur. J. Drug. Metab. Pharmacokinet.* 12: 49–57
- Fleming, C. M., Branch, R. A., Wilkinson, G. R., Guengerich, F. P. (1992) Human liver microsomal N-hydroxylation of dapsone by cytochrome P4503A4. *Mol. Pharmacol.* 41: 975–980
- Gelber, R., Peters, J. H., Gordon, G. R., Glazko, A. J., Levy, L. (1971) The polymorphic acetylation of dapsone in man. *Clin. Pharmacol. Ther.* 12: 225–238
- Gill, H. J., Tingle, M. D., Park, B. K. (1995) N-hydroxylation of dapsone by multiple enzyme of cytochrome P450: implication for inhibition of haemotoxicity. *Br. J. Clin. Pharmacol.* 40: 531–538
- Gordon, G. R., Peter, J. H., Ghoul, D. C., Murray, J. F., Levy, L., Biggs, J. T. (1975) Disposition of dapsone and monoacetyldapsone in rats (39062). *Proc. Soc. Exp. Biol. Med.* 150: 485–492
- Grindulis, K. A., McConkey, B. (1984) Rheumatoid arthritis, the effect of treatment with dapsone on haemoglobin. *J. Rheumatol.* 11: 776–778
- Hein, D. W. (1988) Acetylator genotype and arylamine-induced carcinogenesis. *Biochem. Biophys. Acta* 948: 37–66
- Irshaid, Y., Adedoyin, A., Lotze, M., Branch, R. A. (1994) Monoacetyldapsone inhibition of dapsone N-hydroxylation by human and rat liver microsomes. *Drug Metab. Dispos.* 22: 161–164
- Irshaid, Y., Branch, R., Adedoyin, A. (1996) Metabolic interaction of putative cytochrome P4503A substrates with alternative pathways of dapsone metabolism in human liver microsomes. *Drug Metab. Dispos.* 24: 164–171
- Israïli, Z. H., Cucinell, S. A., Vaught, J., Davis, E., Lesser, J. M., Dayton, P. G. (1973) Studies of the metabolism of dapsone in man and experimental animals: formation of N-hydroxy metabolites. *J. Pharmacol. Ther.* 187: 138–151
- Kinirons, M. K., O'Shea, D., Downing, T. E., Fitzwilliam, A., Joellenbeck, L., Groopman, J. D., Wilkinson, G. R., Wood, A. J. J. (1993) Absence of correlations among three putative in vivo probes of human cytochrome P4503A activity in young healthy men. *Clin. Pharmacol. Ther.* 54: 621–629

- Lee, B. L., Wong, D., Benowitz, N. L., Sullam, P. M. (1993) Altered patterns of drug metabolism with acquired immunodeficiency syndrome. *Clin. Pharmacol. Ther.* 53: 529–535
- Lowry, O. H., Rosebrough, N. J., Farr, A. L., Randall, R. J. (1951) Protein measurement with Folin phenol reagent. *J. Biol. Chem.* 193: 265–275
- Lu, A. Y. H., Levin, W. (1972) Partial purification of cytochrome P-450 and cytochrome P-448 from rat liver microsomes. *Biochem. Biophys. Res. Commun.* 46: 1334–1339
- May, D. G., Porter, J. A., Utrecht, J. P., Wilkinson, G. R., Branch, R. A. (1990) The contribution of N-hydroxylation and acetylation to dapsone pharmacokinetics in normal subjects. *Clin. Pharmacol. Ther.* 48: 619–627
- Mitra, A. K., Thummel, K. E., Kalthorn, T. F., Kharasch, E. D., Unadkat, J. D., Slattery, J. T. (1995) Metabolism of dapsone to its hydroxylamine by CYP2E1 in vitro and in vivo. *Clin. Pharmacol. Ther.* 58: 556–566
- Orzech, C. E., Nash, N. G., Daley, R. (1976) Dapsone. In: Florey, K. (ed.) *Analytical Profiles Of Drug Substances*. Academic Press, New York, pp 88–114
- Palamanda, J. R., Hickman, D., Ward, A., Sim, E., Romkes-Sparks, M., Unadkat, J. D. (1995) Dapsone acetylation by human liver arylamine N-acetyltransferases and interaction with antiopportunistic infection drugs. *Drug Metab. Dispos.* 23: 473–477
- Pochopin, N. L., Charman, W. N., Stella, V. J. (1994) Pharmacokinetics of dapsone and amino acid prodrugs of dapsone. *Drug Metab. Dispos.* 22: 770–775
- Poulsen, A., Hultberg, B., Thomsen, K., Wantzin, G. L. (1984) Regression of Kaposi's sarcoma in AIDS after treatment with dapsone. *Lancet* 1: 560
- Powell, R. D., DeGowin, R. L., Bennet Eppes, R., McNamara, J. V., Carson, P. E. (1967) The antimalarial and hemolytic properties of 4,4'-diaminodiphenylsulfone (DDS). *Int. J. Lepr.* 35: 590–594
- Sonderfan, A. J., Arlotto, M. P., Dutton, D. R., McMillen, S. K., Parkinson, A. (1987) Regulation of testosterone hydroxylation by rat liver microsomal cytochrome P-450. *Arch. Biochem. Biophys.* 255: 27–41
- Vage, C., Svensson, C. K. (1994) Evidence that the biotransformation of dapsone and monoacetyldapsone to their respective hydroxylamine metabolites in rat liver microsomes is mediated by cytochrome P450 2C6/2C11 and 3A1. *Drug Metab. Dispos.* 22: 572–577
- Vage, C., Saab, N., Woster, P. M., Svensson, C. K. (1994) Dapsone-induced hematological toxicity: comparison of the methemoglobin-forming ability of hydroxylamine metabolites of dapsone in rat and human blood. *Toxicol. Appl. Pharmacol.* 129: 309–316
- Williams, J. A., Chenery, R. J., Hawksworth, G. M. (1994) Induction of CYP3A enzymes in human and rat hepatocyte cultures. *Biochem. Soc. Trans.* 22: 131S
- Zaher, H., Svensson, C. K. (1994) Glucocorticoid induction of hepatic acetyl coa: Arylamine N-acetyltransferase activity in the rat. *Res. Commun. Chem. Path. Pharmacol.* 83: 195–208
- Zuidema, J., Hilbers-Modderman, E. S. M., Merkus, F. W. H. M. (1986) Clinical pharmacokinetics of dapsone. *Clin. Pharmacokinet.* 11: 299–315